

Proteomics of HCV virions reveals an essential role for the nucleoporin Nup98 in virus morphogenesis

Marion Lussignol^a, Martina Kopp^{b,1}, Kelly Molloy^c, Gema Vizcay-Barrena^d, Roland A. Fleck^d, Marcus Dorner^{b,e}, Kierstin L. Bell^b, Brian T. Chait^c, Charles M. Rice^{b,2}, and Maria Teresa Catanese^{a,b,2}

^aDepartment of Infectious Diseases, King's College London, London SE1 9RT, United Kingdom; ^bCenter for the Study of Hepatitis C, Laboratory of Virology and Infectious Disease, The Rockefeller University, New York, NY 10065; ^cLaboratory of Mass Spectrometry and Gaseous Ion Chemistry, The Rockefeller University, New York, NY 10065; ^dCentre for Ultrastructural Imaging, King's College London, London SE1 9RT, United Kingdom; and ^eSection of Virology, Imperial College London, London W2 1PG, United Kingdom

Edited by Ralf Bartenschlager, Heidelberg University, Heidelberg, Germany, and accepted by the Editorial Board January 14, 2016 (received for review September 23, 2015)

Hepatitis C virus (HCV) is a unique enveloped virus that assembles as a hybrid lipoviral particle by tightly interacting with host lipoproteins. As a result, HCV virions display a characteristic low buoyant density and a deceiving coat, with host-derived apolipoproteins masking viral epitopes. We previously described methods to produce high-titer preparations of HCV particles with tagged envelope glycoproteins that enabled ultrastructural analysis of affinity-purified virions. Here, we performed proteomics studies of HCV isolated from culture media of infected hepatoma cells to define viral and host-encoded proteins associated with mature virions. Using two different affinity purification protocols, we detected four viral and 46 human cellular proteins specifically copurifying with extracellular HCV virions. We determined the C terminus of the mature capsid protein and reproducibly detected low levels of the viral nonstructural protein, NS3. Functional characterization of virion-associated host factors by RNAi identified cellular proteins with either proviral or antiviral roles. In particular, we discovered a novel interaction between HCV capsid protein and the nucleoporin Nup98 at cytosolic lipid droplets that is important for HCV propagation. These results provide the first comprehensive view to our knowledge of the protein composition of HCV and new insights into the complex virus–host interactions underlying HCV infection.

enveloped virus | Flaviviridae | virion proteomics | virus–host interactions | nucleoporin

Compositional studies of virions provide powerful clues for understanding the functions of viral proteins; assembly and entry pathways; and, more broadly, mechanisms of virus–host interactions. Increasingly sensitive MS techniques have enabled the detection of viral and cellular proteins that are incorporated in virions even at very low levels (1).

Hepatitis C virus (HCV) is a positive-sense ssRNA virus of the Flaviviridae family. This bloodborne pathogen causes chronic liver infection that develops into cirrhosis and hepatocellular carcinoma and is the leading indication for liver transplantation. Over 185 million people are chronically infected with HCV (2). Despite great advances in the ability to study this virus *in vitro*, significant gaps remain in our understanding of the infectious particle and the virus–host interactions required for HCV propagation.

The protein composition of HCV is not known. Although the capsid protein, Core, and the E1 and E2 envelope glycoproteins are thought to be the major constituents of the virion, it remains to be determined if nonstructural viral proteins are packaged as well. A growing body of literature suggests that cellular proteins are important components of HCV. Indeed, this virus closely associates with LDL and very-LDL components, forming a chimeric lipoviral particle (LVP). Biochemical and ultrastructural studies demonstrated that infectious HCV particles are coated with endogenous apolipoproteins that play key roles in viral attachment and entry, explaining the higher infectivity of lipoprotein-associated HCV (2).

The heterogeneous size and appearance of extracellular HCV, ranging from 40 to >100 nm in diameter, suggests that the set of

associated proteins (both viral and cellular), as well as their stoichiometry, might vary across the virion population. Additionally, the specific infectivity of HCV changes according to the cell system/host that the virus is produced in, highlighting a strong contribution of the host to the makeup of the virus particles (2). Therefore, a proteomic analysis of HCV represents an attractive means of discovering novel virus–host interactions with possible implications for understanding exploitation/subversion strategies that this chronic virus uses to persist within the host.

We recently described two methods for producing and affinity-purifying high titers of cell culture-derived HCV (HCVcc) that enabled ultrastructural analysis of HCV virions (3). The first was based on the construction of an infectious clone with tags fused at the N terminus of E2, whereas the second relied on the use of potent HCV-neutralizing Abs.

In this study, we used both affinity purification approaches to perform proteomic analysis of extracellular HCV virions. We established that Core¹⁷⁷ (amino acids 1–177) is the form incorporated in mature HCV particles and detected a number of virion-associated viral and cellular proteins. Functional characterization of HCV-associated cellular proteins identified new host factors, including a nuclear pore complex (NPC) protein, that participate in HCV infection.

Significance

Virion proteomics represents a powerful and unbiased approach to gain insights into the process of virus assembly and the host factors important for infection. For hepatitis C virus (HCV), it is known that infectious virions are assembled alongside endogenous lipoproteins to give rise to a chimeric lipoviral particle. Host-derived apolipoproteins coat the exterior of circulating particles, making for a veiled pathogen. The protein composition of HCV remains, however, undefined. Here, using MS, we identified novel viral and cellular proteins specifically associated with HCV virions and discovered an essential interaction between the capsid protein and the nucleoporin Nup98 that is required for virion biogenesis.

Author contributions: B.T.C., C.M.R., and M.T.C. designed research; M.L., M.K., K.M., G.V.-B., M.D., K.L.B., and M.T.C. performed research; M.L., M.K., K.M., G.V.-B., R.A.F., M.D., K.L.B., B.T.C., C.M.R., and M.T.C. analyzed data; and M.L. and M.T.C. wrote the paper.

Conflict of interest statement: This paper discusses hepatitis C virus research and tools that were developed in academia and licensed to Apath, LLC, a company in which C.M.R. has equity interest.

This article is a PNAS Direct Submission. R.B. is a guest editor invited by the Editorial Board.

¹Present address: Amgen, Thousand Oaks, CA 91320.

²To whom correspondence may be addressed. Email: maria.catanese@kcl.ac.uk or ricec@mail.rockefeller.edu.

This article contains supporting information online at www.pnas.org/lookup/suppl/doi:10.1073/pnas.1518934113/-DCSupplemental.

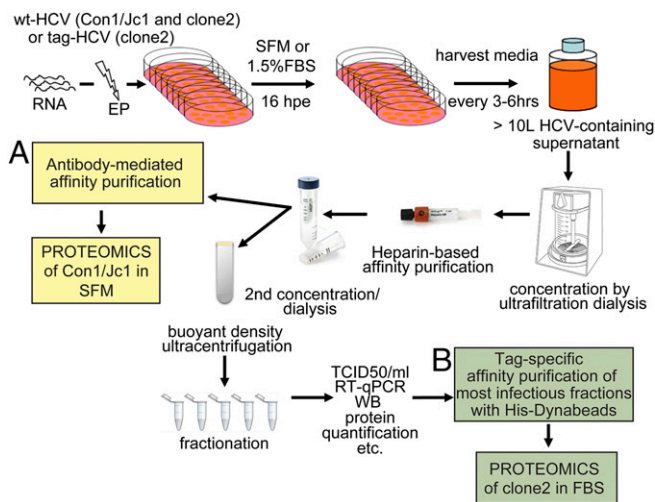


Fig. 1. HCV purification flow chart. Schematic description of the steps used to purify extracellular HCV virions. (A) Con1/Jc1 virus produced in SFM was affinity purified using HCV-neutralizing antibodies prior to proteomics analysis. (B) Tag-clone 2 produced in FBS-containing media was sedimented over a buoyant density gradient and affinity purified with His-Dynabeads. Imidazole-eluted material was subjected to MS, hpi, hours postinfection; qPCR, quantitative PCR; TCID₅₀, 50% tissue culture infectious dose; WB, Western blot.

Results

Purification of Extracellular HCV Virions. Several challenges hampered compositional studies of patient-derived virus or HCV grown in primary hepatocyte cultures. These challenges include the presence of neutralizing Abs in the plasma of infected patients that interfere with the isolation of circulating virions; the high background from serum proteins; and the limited availability, prohibitive costs, and short survival of primary human hepatocytes in cell culture, as well as their low permissiveness to HCV infection. In contrast, large volumes of HCVcc-containing supernatants can be produced in serum-free or low serum-containing media, and viral envelope proteins can be tagged to facilitate virion affinity purification. Large-scale electroporations of HCV RNA into Huh-7.5.1 hepatoma cells were carried out, and cell supernatants were harvested every 3–6 h up to 120 h postelectroporation and stored at 4 °C to minimize temperature-dependent inactivation of HCV (Fig. 1). Between 12 and 15 L of HCV-containing media was produced and concentrated in a nitrogen-pressurized ultrafiltration cell using low protein binding membranes with a molecular mass cutoff of 100 kDa that retained >85% of the viral infectivity (Fig. S1C and Table S1). Two sequential affinity purification steps were used to enrich for envelope-containing particles. The first one relied on a high-affinity interaction between heparin and E2. Although the heparin-eluted material contained less than 50% of the input viral genomes, a striking increase in the specific infectivity [infectious units (IU) per genome RNAs] of the particles was noted (from ~1:4,000 for the input material to 1:5 after heparin purification; Fig. S1B and C and Table S1). The enhanced infectivity suggests that the heparin purification step eliminates noninfectious RNA-containing particles and may additionally remove HCV inhibitors. The heparin column also removed >95% of the protein contaminants present in the concentrated culture supernatant (Fig. S1A). The second affinity purification step consisted of either Ab- or tag-mediated capture of envelope containing HCV particles. In the first case, a Con1/Jc1 virus with five adaptive mutations was produced in serum-free media (SFM), concentrated, heparin-purified, and incubated with a potent HCV-neutralizing Ab that recognizes a discontinuous epitope encompassing E1 and E2 (AR4A) (4) (Fig. 1A). For tag-mediated affinity purification, we used a J6/JFH1 clone 2 infectious genome with a six-histidine (6× His) tag and two copies of a

streptavidin tag II fused to the N terminus of E2 (tag-clone 2) (3) that was harvested in 1.5% FBS (Fig. 1B). Tandem affinity purification using His-Dynabeads (Invitrogen) and Streptactin beads (IBA Lifesciences) was attempted but proved unsuccessful. This result might be partly due to particle aggregation postelution (Fig. S1F). His-Dynabeads resulted in lower background than MagStrep beads and were therefore used for tag-mediated virion purification (3). Production of HCV in FBS-containing media yielded higher titer stocks than SFM. Moreover, tag-specific purification methods captured more virions compared with Abs targeting HCV glycoproteins (3) (Fig. 2A). As a result, tag-HCV, but not Con1/Jc1, was subjected to buoyant density fractionation before the second affinity capture step (Fig. 1). Several gradient solutions were tested to achieve best separation of HCV virions from protein contaminants while preserving their infectivity. Iodixanol gradients recovered >90% of the input infectivity in three fractions (Fig. S1E).

Compositional Analysis of HCV Virions by MS. Transmission EM of negatively stained purified virions, used as input material for proteomics analysis, revealed intact particles (Fig. 2A and B). Constituent proteins in HCV-enriched samples were resolved by SDS/PAGE and stained with Coomassie (Fig. 2C and D).

Viral proteins identified in purified HCV virions. As a first step, selected gel regions where Core, E1, and E2 are expected to migrate (~21 kDa, 35 kDa, and 70 kDa, respectively) were analyzed by liquid chromatography (LC)/MS to determine whether the purification protocols yielded sufficient material to detect the major HCV structural components. Both purification methods led to the identification of Core, E2, and the viral protease nonstructural 3 (NS3) (Table 1 and Fig. S2C). Table 1 lists the number of observed peptides and the percentage of sequence coverage of the protein (corrected for peptides unlikely to be observed by MS). The statistical score associated with the match, $\log(e)$, is also noted. Core displayed the highest relative abundance among the viral proteins using both purification methods, based on the number of unique

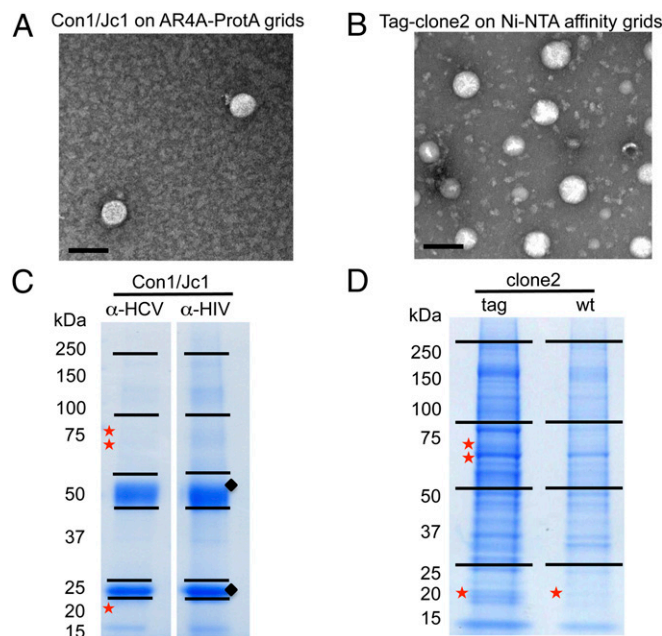


Fig. 2. Analysis of purified HCV virions. (A and B) Transmission EM images of purified HCV particles used for proteomics studies. (Scale bars, 100 nm.) (C and D) Coomassie staining of SDS/PAGE gels subjected to proteomics analysis. Stars indicate the slices where E2, NS3, and Core (top to bottom) were detected; diamonds show the heavy and light Ab chains. Ni-NTA, nickel-nitrilotriacetic acid; wt, wild type.

Table 1. Viral proteins in purified HCV virions

Protein	MS data	Tag-HCV	Wt-HCV	α -HCV	α -HIV
E2	Log (e)	-23	—	-18	—
	Seq cov corr	34	—	35	—
	Unique peps	3	—	3	—
	Spectra	6	—	6	—
Core	Log (e)	-130	-9	-94	—
	Seq cov corr	85	14	36	—
	Unique peps	13	1	9	—
	Spectra	41	2	32	—
NS3	Log (e)	-3.7	—	-3.4	—
	Unique peps	1	—	1	—
	Spectra	2	—	1	—
	Sequences	SIDFIPVETLDVVTR		APITAYAQQTR	

peps, peptides; Seq cov corr, corrected sequence coverage; Wt, wild type.

and total peptides and the sequence coverage achieved. Overall, the sample produced in SFM resulted in a lower LC/MS signal for viral proteins. This result is in agreement with the EM images showing fewer virions in the input material (Fig. 2A). Digestion of virion-associated Core with trypsin resulted in the identification of peptides ending with Arg or Lys, as expected, with the exception of the most C-terminal peptide, which ended with Phe (Fig. 3 and Fig. S2A). To exclude that this cleavage was due to nonspecific trypsin activity, the same sample was digested with Asp-N, with similar results (Fig. S2B). The C terminus of the mature Core protein is produced by the host protease, signal peptide peptidase (SPP), but the form present in mature virions has not been determined (5). Our results indicate that virion-incorporated Core is cleaved at Phe-177. Because E2 is a heavily glycosylated protein, preliminary LC/MS sensitivity tests were conducted using a recombinant soluble E2 ectodomain (6). The identification of unique E2 peptides and total spectra was dose-dependent, with six unique peptides retrieved using the highest amount of purified protein (70 fmol) and a detection limit of ~ 4 fmol (Fig. S3C). Three of these peptides were also detected from mature virions, using either purification approach (Table 1 and Fig. S3G). In the absence of peptide N-Glycosidase F (PNGase F) treatment, no peptides with N-linked glycans were identified, in agreement with previous studies (6). Given the lower amount of input material for the virus preparation in SFM, the gel slices of the Con1/Jc1 sample were cut in two and peptides were extracted with or without in-gel PNGase F digestion. Deglycosylation increased the sensitivity of detection for E2 from three to four unique peptides

A MSTNPKPQRKTKRNTNRRPQDVKEPGGGQIVGGVYLLPBRGPRLGVRATRKTSER
SQPRGRROPIPKDRRSTGKSWGEPGYPWPLYGNEGLGWAGWLLSPRGSRSVWG
NDPDRHRSRNVGKVIDTLTCGFADLMGYIPVVGAPLGGVARALAHGVRVLEDGVNE
ATGNLPGCSFSIFLLALLSCITTPVSA

B 

Fig. 3. Identification of the C terminus of mature Core in extracellular HCV virions. (A) Amino acid sequence of Core corresponding to residues 1–191 of the J6 HCV polyprotein, genotype 2a. The underlined sequences were identified in the database search. Trypsin cleavage sites are shown in bold, whereas the most C-terminal peptide cleavage site is shown in red. (B) Schematic representation of the junction between Core and E1. The predicted sequence and calculated protonated masses (MH^+) of clone 2 Core peptide generated by cleavage with exogenous trypsin protease and the host SPP are indicated in red and match the observed data. Full-length Core (191 aa) is generated by cleavage of the signal peptidase (SP), whereas mature Core is produced by SPP-mediated cleavage at position 177.

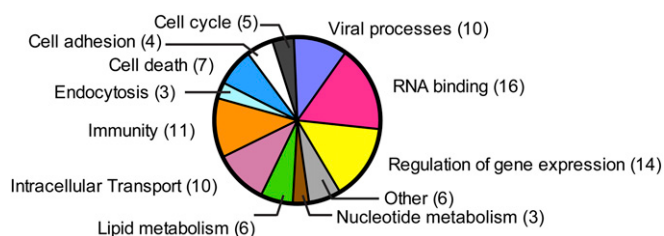


Fig. 4. Functional classification of host proteins in HCV virions according to their known cellular functions.

for the enzyme-treated slice, with the additional peptide containing an NXT glycosylation motif (Fig. S3G). Although no E1 peptides were detected in PNGase F-treated virus preparations, E1 incorporation in virions could be inferred by the fact that the HCV-specific Ab used for the purification recognizes a conformational epitope encompassing E1/E2 (AR4A) (4). Interestingly, the 70-kDa gel region analyzed for E2 detection also contained peptides of the viral protease NS3. Three and one NS3 peptides were retrieved using both tag- and Ab-mediated virus capture, respectively, suggesting that NS3 may be a virion component (Table 1).

Cellular proteins identified in purified HCV virions. Tag-mediated purification, although successful for isolating intact virions, resulted in high protein background with significant contamination from FBS-derived proteins, hampering the identification of host proteins that specifically associate with HCV. Therefore, we used the HCV-neutralizing Ab AR4A as an alternative approach to purify HCV virions. As a negative control, the same amount of infectious particles was incubated with an HIV-specific Ab (B6). A protein was considered a candidate virion-associated factor if it satisfied all of the following criteria: (i) It is not a known exogenous contaminant, such as keratin; (ii) the log(e) score value does not exceed the log(e) score value of any protein identified from the decoy database of reversed protein sequences; and (iii) both the main protein candidate identified by X!Tandem and its homologs had zero spectrum counts in the corresponding control sample. In total, 46 human proteins were specifically isolated with HCV virions (Table S2). These host factors were grouped into functional categories, including RNA binding, regulation of gene expression, immunological and viral processes, intracellular transport, lipid metabolism, and endocytosis (Fig. 4 and Table S3). Although apolipoproteins (apo) are known components of LVPs, they are not in the list of HCV-associated host factors according to the stringent inclusion criteria, because some peptides were also found in the control lane. Nevertheless, human apoE, apoB-100, apoA-II, apo-CII, and apo-CIII were enriched in purified HCV (Table S4).

Validation of Virion-Associated Host Proteins. To corroborate the proteomics data, 12 candidate cellular proteins were validated in follow-up studies by RNAi (Table 2). These host factors were prioritized based on the following criteria: (i) observed peptides ($n \geq 3$); (ii) $\log(e) \leq -7$; and (iii) previous implication in HCV or other viral infections, based on PubMed search. The siRNA smart pools targeting the HCV genome and the entry receptor CD81 were used as positive controls for inhibition of viral infection in our functional assays (Fig. 5). ApoB-100 and ApoA-I siRNAs were also included in the analysis, because we previously demonstrated specific incorporation of these host-derived proteins in infectious HCV particles (3). Two days posttransfection with siRNAs, Huh-7.5 cells were challenged with Con1/Jc1 at a low multiplicity of infection (MOI), and the number of NS5A-positive cells and viral genomes released in the culture media was measured 72 h later by fluorescence-activated cell sorting (FACS) and RT-quantitative PCR, respectively (Fig. 5). Therefore, this assay mainly looked at the impact of protein

Table 2. HCV-associated cellular proteins identified by MS and selected for follow-up studies

No.	Identifier	Gene name	Protein name	Log (e)	No. of spectra	Molecular mass, kDa	Gel slice
1	ENSP00000351416	ANKRD17	Ankyrin repeat domain 17	-54.9	9	274.1	A
2	ENSP00000448366	SCYL2	SCY1-like 2	-18.1	3	77	A
3	ENSP00000392423	RELN	Reelin	-7.9	3	388.1	A
4	ENSP00000376899	PTGFRN	Prostaglandin F2 receptor inhibitor	-54.3	12	98.5	B
5	ENSP00000295598	ATP1A1	ATPase, Na ⁺ /K ⁺ transporting, alpha-1 polypeptide	-27.4	5	112.8	B
6	ENSP00000316032	NUP98	Nucleoporin 98kDa	-17.3	6	195.7	B
7	ENSP00000367122	SLC3A2	Solute carrier family 3, member 2	-23.8	4	68	C
8	ENSP00000264883	NUP54	Nucleoporin 54 kDa	-14.3	6	55.4	C
9	ENSP00000387282	AGFG1	ArfGAP with FG repeats 1	-7.7	3	60.7	C
10	ENSP00000260130	SDCBP	Syndecan binding protein (syntenin)	-10.7	3	32.4	E
11	ENSP00000221566	SGTA	Small glutamine-rich tetratricopeptide repeat-containing, alpha	-10.3	3	34	E
12	ENSP00000227525	TMEM109	Transmembrane protein 109	-35.2	15	26.2	G

ArfGAP, GTP-ase activating protein for ADP-ribosylation factors; FG, Phe-Gly.

down-regulation on secondary rounds of infection, determining a cumulative effect of the host factors on HCV propagation rather than discriminating between individual steps of the virus life cycle. Cell viability was measured by FACS from the same set of samples at the time of harvesting (Fig. S4B). mRNA expression levels of the targeted host factors were measured by real-time RT-PCR to confirm decreased expression of the intended gene by specific siRNAs (Fig. S4C). A striking decrease in the number of infected cells (Fig. 5A and C and Fig. S44) and extracellular viral genomes (Fig. 5B and C) was observed in cells silenced for the nucleoporin Nup98. This decrease was paralleled by a two-log reduction in viral titers, when cell culture media derived from siRNA-transfected cells was inoculated onto naive Huh-7 cells (Fig. 5D). Interestingly, silencing of SCYL2 and PTGFRN resulted in a 75% and 60% increase in HCV infection, respectively, suggesting an antiviral activity for these host factors. Finally, moderate inhibition of infection (~50%) was observed in cells where endogenous SLC3A2, TMEM109, ATP1A1, and SGTA were down-regulated.

Nup98 Interacts with Core and Relocalizes to Cytosolic Lipid Droplets in Infected Cells. Given the profound inhibition of infection upon Nup98 silencing, we further investigated the role of this protein in HCV biology. Because Nup98 was found in HCV particles, we tested whether it bound to virion structural components. We showed that Core specifically coimmunoprecipitates with endogenous Nup98 (Fig. 6A). In physiological conditions, Nup98 localizes at the nuclear envelope, being a component of the NPC (7). Therefore, the role of Nup98 in HCV infection and its packaging into virions was unexpected considering that HCV replicates in the cytoplasm. To understand where the interaction between Nup98 and Core occurs, we performed immunofluorescence and electron microscopy (iEM) studies of infected Huh-7.5 cells. Differences in Nup98 subcellular distribution were observed at early vs. late stages of infection. Initially, Nup98 staining is comparable to uninfected cells, mainly localizing at the nuclear envelope (Fig. S5A and D). In contrast, 6 d postinfection, Nup98 is enriched on large, round cytoplasmic structures, where Core also localizes (Fig. S5A and B). Core is known to accumulate on cytosolic lipid droplets (cLDs), cytoplasmic organelles for lipid storage, before being used for the nucleation of viral capsids (8). To confirm that Core and Nup98 were colocalizing on cLDs, we used the Tokuyasu (9) technique for immunolabeling of cryosections. The expected staining of Core on the surface of cLDs was observed. Furthermore, Nup98 was shown to relocalize to cLDs while retaining its physiological localization at the nuclear envelope (Fig. 6B). Costaining with Core- and Nup98-specific Abs by iEM confirmed that the two proteins

colocalize on the surface of cLDs in infected cells (Fig. 6B and Fig. S5C).

Nup98 Is Required for HCV Morphogenesis. To dissect the role of Nup98 in HCV biology, Huh-7.5 cells were transfected with lentiviral particles encoding either irrelevant shRNA (shIRR) or Nup98-specific shRNA (shNup98) (Fig. 7). The two cell lines were compared using viral assays that looked at specific steps of the HCV life cycle. HCV infection was impaired in cells where Nup98 protein expression was down-regulated, as shown by the reduction of intracellular Core levels (Fig. 7A). The negative impact of Nup98 silencing on infection was overcome in a dose-dependent manner by using higher MOI, suggesting that the block is not at the level of

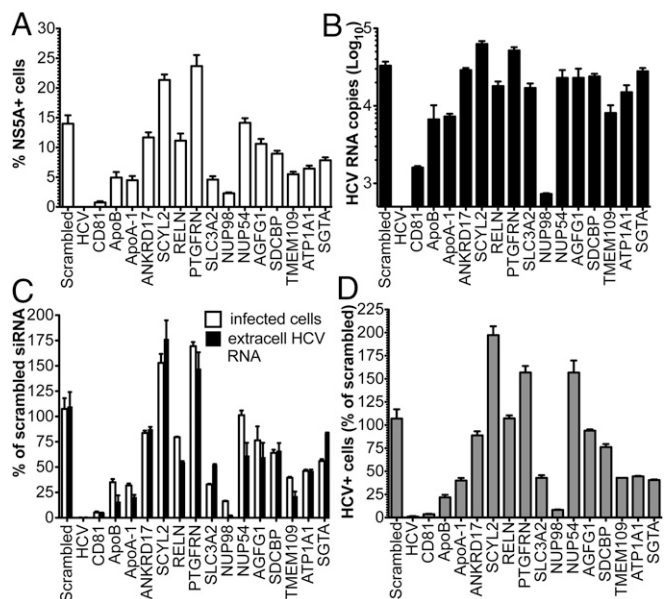


Fig. 5. Validation of cellular proteins incorporated in HCV virions by RNAi. Huh-7.5 cells were transfected with siRNA smart pools against the indicated molecules and infected 48 h later with Con1/Jc1 at low MOI (0.05). (A and C) Percentage of HCV⁺ cells was determined 3 d postinfection (dpi) by NS5A staining and FACS analysis (white bars). (B and C) Number of HCV RNA genomes released in the cell media was quantified by RT-quantitative PCR (black bars). (D) Infectivity of HCV particles produced by siRNA-transfected cells was assessed by inoculating equal volumes of cell culture media on naive Huh-7 cells. The number of NS5A⁺ cells was determined by FACS 3 dpi. In C and D, data are expressed as a percentage of scrambled siRNA.

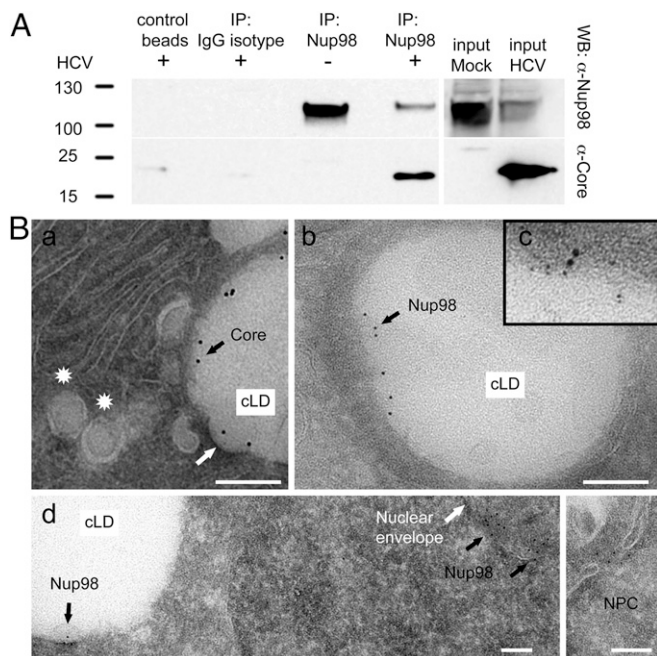


Fig. 6. Nup98 interacts with Core and relocates to cLDs in infected cells. (A) Cell lysates from naive and clone 2-infected Huh-7.5 cells (6 dpi) were immunoprecipitated (IP) with anti-Nup98 Ab. Beads without Ab (control beads) or conjugated to isotype-matched IgG served as negative controls. Immunoblot analysis with anti-Nup98 and anti-Core Abs is shown. (B) Huh-7.5 cells infected with clone 2 for 4 d were cryosectioned and stained with Abs to Core (a), Nup98 (b and d), or both (c). Representative iEM images are shown. (a) Core is enriched on cLDs juxtaposed to endoplasmic reticulum (ER) membranes. Membrane curvature may represent a nucleocapsid budding event (white arrow). Spherical particles within vacuoles may be HCV virions at early maturation stage (stars). (c) Costaining with Core-specific (12 nm) and Nup98-specific (6 nm) Abs. (d) Low-magnification image shows the expected localization of Nup98 on both sides of the nuclear envelope, in the central channel of the NPC (*Inset*), and the additional presence of Nup98 on cLD. (Scale bars, 100 nm.)

virus entry or early steps of infection (Fig. 7B). Accordingly, using a luciferase-reporter Jc1 virus, we showed that HCV replication and translation were comparable between shIRR and shNup98 cells (Fig. 7C). In contrast, the amount of both intracellular and extracellular infectious particles produced by shNup98 cells was reduced by 50% and 90%, respectively, compared with control cells, indicating a role for Nup98 in the late steps of virion biogenesis (Fig. 7D).

Discussion

In the past decade, substantial progress in growing HCVcc has been made by using highly permissive cell lines and by selecting more fit viral genomes with adaptive mutations (10). Nevertheless, HCVcc titers remain in the range of 10^5 – 10^6 50% tissue culture infectious dose per milliliter (TCID₅₀/ml), which is ~100- to 1,000-fold less than other enveloped viruses for which protein composition has been determined (1). If higher virus yields are achieved when serum is added to the culture media, contamination by highly abundant serum proteins compromises the ability to detect cellular proteins that are anticipated to be packaged into HCV virions in low copy numbers (Fig. 2). Furthermore, poor stability of virions makes the purification process extremely time-sensitive, limiting the number of purification steps that can be undertaken before most of the infectivity is lost (11). Finally, propensity to forming aggregates has been observed, preventing tandem affinity purification approaches (Fig. S1).

We undertook appropriate complementary approaches to compositional studies of extracellular HCV virions, using different viral genomes and affinity purification methods. Up to 15 L of

virus-containing supernatant was produced for this study, and culture media were harvested frequently and stored at 4 °C to prevent virus inactivation (Fig. 1). More infectious virus particles (approximately 5- to 10-fold) were being produced using FBS-containing media, and these virions were better captured using tag-mediated rather than Ab-mediated purification methods (3). Accordingly, a better sequence coverage of viral proteins was achieved by LC/MS using HCV samples produced in serum. Conversely, HCV isolation via glycoprotein-specific Abs was more effective with preparations in SFM and resulted in significantly cleaner virion pull downs (Fig. 2). However, lower viral titers were achieved in SFM, hampering further fractionation approaches by ultracentrifugation.

Despite these differences, both approaches led to the identification of the same set of viral proteins, with Core displaying the highest sequence coverage (Table 1). Previous studies have shown that Core is cleaved by SPP at Phe-177 and that amino acids 1–177 of the protein are necessary and sufficient for HCV infectivity (5, 12). Using purified HCV virions fractionated over buoyant density gradient, we now determined that the C terminus of Core packaged in infectious particles is Phe-177 (Fig. 3 and Fig. S2).

In addition to the expected structural viral proteins, the protease NS3 was identified in virions produced in FBS as well as SFM, using different purification methods (Table 1 and Fig. S2C). A possible explanation for this finding may be that incoming HCV particles would benefit from having a viral protease that can promptly inactivate cytoplasmic viral sensors upon capsid uncoating, before the formation of the membranous web. Alternatively, given its role in HCV assembly, NS3 may be incorporated in virions by proximity (2). The low signal compared with Core and E2 is consistent with the expectation of the protease not being incorporated in high copy numbers.

The present study reveals an intimate interplay between HCV and the host in the makeup of infectious particles, with 46 potential

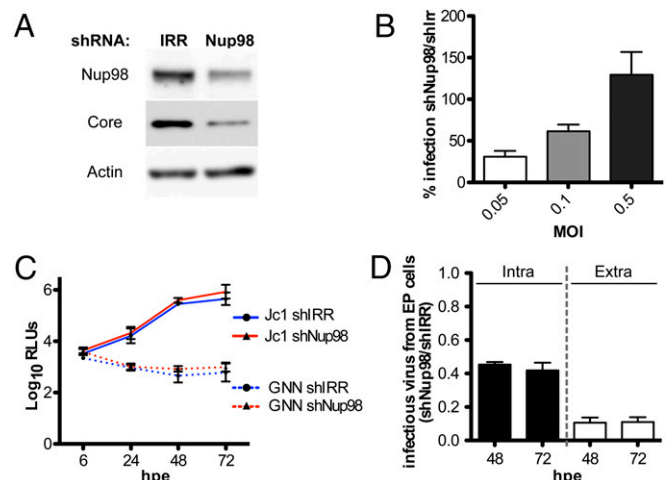


Fig. 7. Impact of Nup98 on the HCV life cycle. (A) Immunoblot analysis showing Nup98 and Core expression in Huh-7.5 cells expressing either shIRR or shNup98 3 dpi with HCV clone 2. (B) shIRR or shNup98 cells were infected with clone 2 at the indicated MOI for 3 d, and the percentage of N55A⁺ cells was determined by FACS analysis. Data are expressed as the percentage of infection measured in shNup98 compared with shIRR. (C and D) shIRR and shNup98 cells were electroporated with Jc1FLAG2(p7-nsGluc2A) and Jc1FLAG2(p7-nsGluc2A)/GNN RNAs. (C) Kinetics of luciferase secretion in cell culture media were measured between 6 and 72 h postelectroporation (hpe) to monitor viral RNA translation and replication. AR4A was added to the culture media at 1 μ g/mL to minimize secondary rounds of infection. (D) Intracellular and extracellular virus harvested from shNup98 and shIRR cells at 48 and 72 hpe was inoculated onto naive Huh-7.5 cells. Infectivity was assessed by luciferase quantification and is shown as the ratio of infection obtained with inocula derived from shNup98 compared with shIRR cells. EP, electroporated.

cellular proteins incorporated into mature virions (Table S2), belonging to a variety of functional classes (Fig. 4 and Table S3). Although it is unclear whether all of these cellular proteins represent true virion components or are only peripherally associated with HCV particles, some of them were previously linked to viral processes (Table S3) and are specifically regulated during HCV infection (13).

Two of these proteins, PTGFRN and SCYL2, display antiviral roles not only against HCV (Fig. 5 and Fig. S44) but also against other pathogens. PTGFRN (also called CD9P-1 or EWI-F) inhibits the ability of hepatocytes to support *Plasmodium* sporozoite infection by interacting with CD81 (14). Interestingly, PTGFRN was shown to be up-regulated in HCV-infected cells (13). The IFN-stimulated gene SCYL2 is a component of clathrin-coated vesicles involved in membrane trafficking between the trans-Golgi and endosomes, and it was shown to restrict HIV release by inhibiting the viral protein Vpu (15). Further investigations will be required to determine how these host factors counteract HCV infection and whether they can be considered bona fide restriction factors.

Conversely, Nup98 displayed the strongest proviral phenotype, with a profound reduction in viral genome release and infectious titers upon silencing (Fig. 5). A previous study identified Nup98 as an important host protein for HCV infection (16). Here, we show that Nup98 is copurified with extracellular HCV virions (Table 2), physically interacts with Core (Fig. 6 and Fig. S5), and is specifically required for late stages of the HCV life cycle (i.e., assembly/maturation) (Fig. 7). Follow-up studies will determine whether Nup98's impact on HCV biogenesis is direct or can also be explained by Nup98 modulation of cellular gene expression.

Nup98 dynamically associates with the NPC, where it regulates nucleocytoplasmic transport of mRNAs and proteins (7). We propose that HCV hijacks Nup98 physiological functions to transport HCV structural components from different cellular compartments, thus coordinating virion morphogenesis. Accordingly, several HCV proteins, including Core, contain functional nuclear localization signal and nuclear export signal sequences that are required to bind cargo proteins and cross the NPC (17). This hypothesis would be in agreement with the model proposed by Neufeldt et al. (16), which suggests the insertion of NPC in the cytoplasm of infected cells to compartmentalize virus replication/assembly. To date, viruses have been described to target the NPC, to cross the nuclear envelope, and/or to control host transcription. In contrast, our proteomics, biochemical, and ultrastructural data suggest a novel mechanism of Nup98 exploitation to aid virus assembly.

In summary, we report the protein composition of extracellular HCV particles. Future studies can address the functional roles that other HCV-associated host factors may fulfill during specific steps of the virus life cycle. These investigations will further our understanding of the host contribution to HCV propagation and pathogenesis.

Materials and Methods

Virion Purification. HCV stocks were created by electroporating viral RNA into Huh-7.5.1 cells (18). Cells were switched to low-serum media [1.5% (vol/vol) FBS] or 5FM 12 h postelectroporation, and virus-containing media were harvested every 3–6 h up to 5 d postelectroporation. Viral supernatants were concentrated in a stirred ultrafiltration cell (Model 8400 with 100-kDa molecular mass cutoff membranes; Millipore) and purified over a heparin column (Hitrap Heparin; GE Healthcare). Heparin-bound HCV was eluted with 0.02 M Tris-HCl (pH 7.4) and 0.5 M NaCl, and dialyzed with PBS1X (Invitrogen Gibco) using Amicon Ultra centrifugation devices (regenerated cellulose, low protein binding capacity with 100-kDa molecular mass cutoff; Millipore). Heparin-eluted Con1/Jc1 was incubated with ProtA-coated magnetic beads (Bio-Adembeads; Ademtech), conjugated to Abs specific to HCV (AR4A) or HIV (B6) envelope glycoproteins, and eluted in SDS buffer. Heparin-eluted clone 2-His/one-strep-tag (tag) and wild-type viruses were fractionated over a 10–40% (wt/vol) iodixanol buoyant density gradient (Optiprep; Sigma) (3). Fractions with the highest infectivity were incubated with His-Dynabeads (Invitrogen) for 1 h at room temperature in the presence of 20 mM imidazole and protease inhibitors. Bound particles were washed with 50 mM imidazole and eluted with 900 mM imidazole (in PBS1X, pH 7.7).

Proteomics Analysis. Gel lanes were sliced in 1-mm intervals, and slices were pooled into six samples. Slices were cubed and destained with 50% (vol/vol) acetonitrile in 50 mM ammonium bicarbonate. To deglycosylate proteins, gel pieces were incubated with 80 μ L of PNGase F (11 units/ μ L; New England BioLabs) in 50 mM sodium phosphate (pH 7.5) at 37 $^{\circ}$ C overnight and then washed four times with water the next day. Proteins were digested overnight in 3.1 ng/ μ L trypsin (Promega) in 25 mM ammonium bicarbonate. Peptides were extracted with 2.5 mg/mL POROS R2 20- μ m beads (Life Technologies) in 5% (vol/vol) formic acid and 0.2% TFA on a shaker at 4 $^{\circ}$ C for 24 h. Digests were desalted on Stage Tips (made in-house with 2 layers of octadecyl C18, Empore 2215), eluted, concentrated by SpeedVac (Thermo Savant, SPD111V), and loaded onto a 75- μ m ID PicoFrit column (New Objective) packed in-house with 6 cm of reverse-phase C18 material (5- μ m particles, 300- Å pores, YMC*Gel ODS-A; YMC). Peptides were gradient-eluted (using 0.1 M acetic acid and 0.1 M acetic acid in 70% (vol/vol) acetonitrile at a flow rate of 200 nL/min) into an LTQ-Orbitrap-XL mass spectrometer (ThermoFisher Scientific) acquiring data-dependent collision-induced dissociation (CID) fragmentation spectra. Using the X!Tandem algorithm, raw data were searched against databases of human, bovine, and HCV protein sequences, as well as a decoy database of reversed protein sequences.

Detailed methods can be found in *SI Materials and Methods*.

ACKNOWLEDGMENTS. We thank Dr. Joseph Marcotrigiano (Rutgers University) for providing soluble E2, Dr. Mansun Law (The Scripps Research Institute) for the AR4A and B6 Abs, and Harishabd Khalsa for assistance with data analysis. We also thank Dr. Michael Rout (The Rockefeller University) and Dr. Beatriz Fountoura (UT Southwestern) for insightful discussions. This work was supported by NIH grants (to C.M.R.), The Greenberg Medical Research Institute, The Starr Foundation, and Public Health Service Grants GM103314 and GM109824 (to B.T.C.). M.L. was supported by departmental start-up funds (King's College London). M.T.C. is the recipient of a Rockefeller University Women & Science Fellowship. Funding for M.K. was provided by the Deutsche Forschungsgemeinschaft.

- Maxwell KL, Frappier L (2007) Viral proteomics. *Microbiol Mol Biol Rev* 71(2):398–411.
- Lindenbach BD, Rice CM (2013) The ins and outs of hepatitis C virus entry and assembly. *Nat Rev Microbiol* 11(10):688–700.
- Catanese MT, et al. (2013) Ultrastructural analysis of hepatitis C virus particles. *Proc Natl Acad Sci USA* 110(23):9505–9510.
- Giang E, et al. (2012) Human broadly neutralizing antibodies to the envelope glycoprotein complex of hepatitis C virus. *Proc Natl Acad Sci USA* 109(16):6205–6210.
- Okamoto K, et al. (2008) Intramembrane processing by signal peptide peptidase regulates the membrane localization of hepatitis C virus core protein and viral propagation. *J Virol* 82(17):8349–8361.
- Whidby J, et al. (2009) Blocking hepatitis C virus infection with recombinant form of envelope protein 2 ectodomain. *J Virol* 83(21):11078–11089.
- Griffis ER, Xu S, Powers MA (2003) Nup98 localizes to both nuclear and cytoplasmic sides of the nuclear pore and binds to two distinct nucleoporin subcomplexes. *Mol Biol Cell* 14(2):600–610.
- Miyanari Y, et al. (2007) The lipid droplet is an important organelle for hepatitis C virus production. *Nat Cell Biol* 9(9):1089–1097.
- Tokuyasu KT (1973) A technique for ultracytometry of cell suspensions and tissues. *J Cell Biol* 57(2):551–565.
- Catanese MT, Dorner M (2015) Advances in experimental systems to study hepatitis C virus in vitro and in vivo. *Virology* 479–480:221–233.
- Ciesek S, et al. (2010) How stable is the hepatitis C virus (HCV)? Environmental stability of HCV and its susceptibility to chemical biocides. *J Infect Dis* 201(12):1859–1866.
- Kopp M, Murray CL, Jones CT, Rice CM (2010) Genetic analysis of the carboxy-terminal region of the hepatitis C virus core protein. *J Virol* 84(4):1666–1673.
- Diamond DL, et al. (2010) Temporal proteome and lipidome profiles reveal hepatitis C virus-associated reprogramming of hepatocellular metabolism and bioenergetics. *PLoS Pathog* 6(1):e1000719.
- Charrin S, et al. (2009) The Ig domain protein CD9P-1 down-regulates CD81 ability to support *Plasmodium yoelii* infection. *J Biol Chem* 284(46):31572–31578.
- Miyakawa K, et al. (2012) Interferon-induced SCYL2 limits release of HIV-1 by triggering PP2A-mediated dephosphorylation of the viral protein Vpu. *Sci Signal* 5(245):ra73.
- Neufeldt CJ, et al. (2013) Hepatitis C virus-induced cytoplasmic organelles use the nuclear transport machinery to establish an environment conducive to virus replication. *PLoS Pathog* 9(10):e1003744.
- Levin A, et al. (2014) Functional characterization of nuclear localization and export signals in hepatitis C virus proteins and their role in the membranous web. *PLoS One* 9(12):e114629.
- Lindenbach BD, et al. (2005) Complete replication of hepatitis C virus in cell culture. *Science* 309(5734):623–626.
- Jones CT, et al. (2010) Real-time imaging of hepatitis C virus infection using a fluorescent cell-based reporter system. *Nat Biotechnol* 28(2):167–171.
- Andrus L, et al. (2011) Expression of paramyxovirus V proteins promotes replication and spread of hepatitis C virus in cultures of primary human fetal liver cells. *Hepatology* 54(6):1901–1912.
- Catanese MT, et al. (2013) Different requirements for scavenger receptor class B type I in hepatitis C virus cell-free versus cell-to-cell transmission. *J Virol* 87(15):8282–8293.